Bioorganic Chemistry 85 (2019) 534–540

Contents lists available at ScienceDirect

Bioorganic Chemistry

journal homepage: www.elsevier.com/locate/bioorg

Design, synthesis and evaluation of D-amino acid-containing peptidomimetics targeting the polo-box domain of polo-like kinase 1

Zhiyan Li[a,b,c], Zhenguo Zhang[a,b,c], Yanhong Chen[a,b,c], Shijun Tang[a,b,c], Tongyuan Lin[a,b,d], Jingfang Huang[b,d], Bo Li[b,d,*], Cheng Jiang[a,b,c,*]

[a] Jiangsu Key Laboratory of Drug Design and Optimization, China Pharmaceutical University, Nanjing 210009, China
[b] Key Laboratory on Protein Chemistry and Structural Biology, China Pharmaceutical University, Nanjing 210009, China
[c] Department of Medicinal Chemistry, China Pharmaceutical University, Nanjing 210009, China
[d] Key Laboratory of Drug Quality Control and Pharmacovigilance, China Pharmaceutical University, Nanjing 210009, China

ARTICLE INFO

Keywords:
Polo like kinase 1
Polo-box domain
Inhibitors
D-amino acid
Anticancer

ABSTRACT

A series of D-amino acid-containing peptidomimetics were designed, synthesized as novel polo-like kinase 1 (Plk1) polo-box domain (PBD) inhibitors based on the reported peptide Plk1 PBD inhibitor. Their inhibitory activity to Plk1, Plk2, and Plk3 PBD were evaluated using our fluorescence polarization (FP) assay. Compound **18** bound to Plk1 PBD with IC_{50} of 0.80 μM and showed nearly no inhibition to Plk2 PBD or Plk3 PBD at 100 μM. Compound **18** induced Hela cells to undergo apoptosis by increasing the ratio of the cells at the G2/M phase by decreasing the neosynthesized proteins in a dose-dependent manner from 50 to 150 μM. Compound **18** showed improved stability in rat plasma compared to L-peptide inhibitor LHSpTA. These novel D-amino acid modified selective Plk1 PBD inhibitors may provide new lead compounds for further optimization.

1. Introduction

The serine/threonine kinase polo-like kinase 1 (Plk1) is a member of the polo-like kinases family which acts as a regulator in the transition through the G2/M checkpoint by influencing the activation of the cell division cyclin 25 homolog C (CDC25C) phosphatase and Cyclin B1 [1,2]. Plk1 has been observed overexpressed in several kinds of human cancers and was often correlated with poor patient prognosis [2]. The inhibition of Plk1 could induce cell apoptosis in a broad spectrum of cancer cell lines [3]. Thus Plk1 was considered as an attractive target in the development of anticancer drug.

Among the five Plks (Plk1-5) identified in mammalian cells, Plk1-4 is composed of a common *N*-terminal catalytic domain and a *C*-terminal regulatory domain containing a consensus S-pS/pT-P/X sequence, named polo-box domains (PBDs) [3,4]. PBD is observed only in the Plks and considered to be involved in auto-regulatory mechanism or sub-cellular localization which is critical for normal Plk function [4,5]. Plk1, Plk2 and Plk3 are closely related while Plk4 is a less related kinase which apparently expressed in different patterns and showed different physiological functions [3,4]. However, Plk2 and Plk3, two most closely related kinases with Plk1, appear to function as oncogenic suppressors [3–5]. Therefore developing Plk1 PBD selective inhibitors represents an effective strategy in the treatment of Plk1-related cancer.

A minimal peptide (PLHSpT, **1**) was identified as an inhibitor with high affinity for Plk1 PBD that blocked Plk1 binding to polo-box-interacting protein 1 (PBIP1), a centromere/kinetochore-associated target [6]. After that, several phosphate peptides and peptidomimetics were reported with enhanced Plk1 PBD binding affinity (Fig. 1, **2–4**) [6–15]. A series of (2*S*, 3*R*)-2-amino-3-methyl-4-phosphonobutanoic acid (Pmab) incorporated peptidomimetic were reported (Fig. 1, **5**) as a phosphatase-stable peptidomimetic with complete retention of inhibitory potency [16].

Although PLHSpT and its derivatives showed excellent binding affinity and selectivity for the Plk1 PBD, they have several issues such as limited bioavailability, and poor plasma stability, et al. [13]. To overcome these weakness, the amino acids of the parental peptide were substituted with unnatural amino acids. These approaches can improve the stability and bioavailability, while maintaining high affinity and selectivity to Plk1 PBD against the closely related Plk2 PBD and Plk3 PBD [13]. D-amino acids are known to enhance the stability of engineered peptides to proteases [17–20]. Based on this, in this study, unnatural D-amino acid was introduced to the peptide aiming for identifying novel and plasma stable Plk1 PBD inhibitors.

* Corresponding authors at: Jiangsu Key Laboratory of Drug Design and Optimization, China Pharmaceutical University, Nanjing 210009, China.
E-mail addresses: libo@cpu.edu.cn (B. Li), jc@cpu.edu.cn (C. Jiang).

https://doi.org/10.1016/j.bioorg.2019.02.022
Received 20 December 2018; Received in revised form 27 January 2019; Accepted 9 February 2019
Available online 11 February 2019
0045-2068/

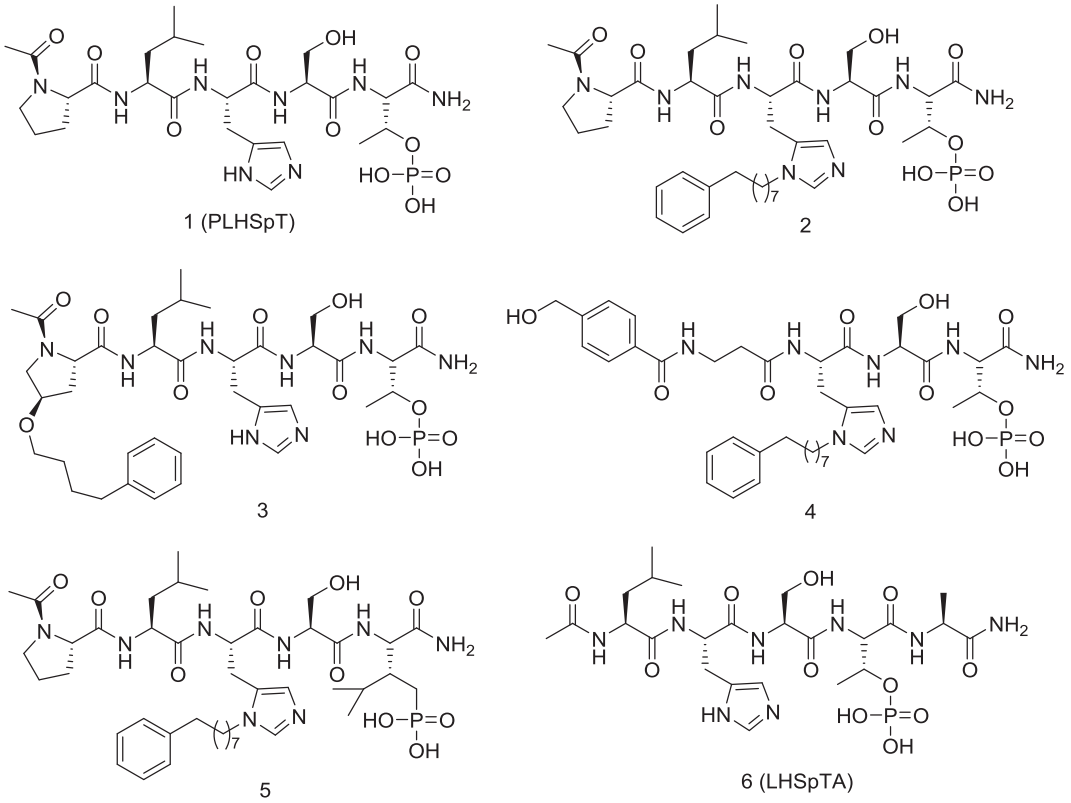

Fig. 1. Representative phosphate peptides and peptidomimetics as Plk1 PBD inhibitors.

2. Results and discussion

2.1. Design, synthesis and screening

In the discovery of PLHSpT, another peptide, LHSpTA (Fig. 1, **6**), was also reported, which has a very similar binding affinity compared to PLHSpT [6]. For easier solid phase peptide synthesis, LHSpTA was selected as a lead compound for modification. Firstly, the L-Leu residue in LHSpTA was replaced by D-Leu and then ^{D}LHSpTA(**7**) was synthesized. The binding affinity of **6** and **7** to Plk1 PBD was evaluated using our optimized fluorescence polarization (FP) binding assay [21]. As shown in Table 1, **6** and **7** showed similar binding affinity to Plk1 PBD. Hence, we further diversified the peptidomimetic **7** skeleton with various substituted aryl fragments at the *N*-terminus, trying to determine other elements critical for the binding affinity of ^{D}LHSpTA derivatives (Table 1).

A series of ^{D}LHSpTA-derived peptidomimetics, with the *N*-terminal D-Leu acylated by L-Pro (the *N*-terminal substitution of PLHSpT), aromatic or nonaromatic ring systems, were synthesized and evaluated for Plk1 PBD inhibition activity as listed in Table 1). Peptidomimetic **8** having an *N*-terminal L-Pro substituent showed about 10 times more potent Plk1 PBD inhibition activity (IC_{50} = 0.80 μM) than the lead **6**. In contrast, peptidomimetic **9–15** acylated by aromatic or nonaromatic ring systems without hetero atom at the *N*-terminal dramatically decreased the binding affinity compared to peptidomimetic **8**. Interestingly, peptidomimetic **16**, **17** and **18** having an *N*-terminal acylated by aromatic heterocycle showed similar potency to **8**. The hetero atom at the *N*-terminal substituent may be essential for the potent Plk1 PBD inhibition activity of the ^{D}LHSpTA-derived peptidomimetics.

2.2. Isoform selectivity

The binding affinity of **8**, **16**, **17** and **18** for Plk2 PBD and Plk3 PBD was evaluated in our FP assay. As shown in Table 1, none of the tested compounds showed binding affinity to Plk2 PBD and Plk3 PBD at 100 μM. The new identified D-amino acid-containing peptidomimetics showed excellent selectivity to Plk1 PBD against Plk2 PBD and Plk3 PBD.

2.3. Cell growth inhibition

The antiproliferative effects of **18** was investigated in HeLa cells. A previous literature reported that the PEGylated version of compound **4** (Plk1 PBD IC_{50} = 0.04 μM) effectively inhibited cell proliferation in a dose-dependent manner with an IC_{50} about 348 μM [13]. This was considered as the drawback of the poor membrane permeability for phosphopeptides [13]. The proliferation rates of HeLa cells incubated in the presence of **18** for 24 h were determined at increasing concentrations (0–200 μM). We observed that **18** inhibited cell survival in a dose-dependent manner with an IC_{50} of 122 μM (Fig. 2). The peptidomimetic **18** showed significant inhibition to the proliferation of HeLa cells at lower concentration even though the binding affinity to Plk1 PBD was 20 times lower than compound **4** *in vitro*.

2.4. Investigation of cell cycle distribution in HeLa cells

The cell cycle analysis was performed to investigate the prevention of proliferation in HeLa cells with the most potent compound **18**. After treatment of HeLa cells with compound **18** for 24 h at indicated concentrations (50, 100 and 150 μM), the cells were fixed and stained with PI, the DNA content was analyzed by flow cytometry. The obtained results were compared with non-treated HeLa cells as control. As shown in Fig. 3**A and 3B**, treatment of HeLa cells with **18** at 50, 100 and 150 μM concentrations increased the percentage of G2/M-phase cells from 12.1% (as control group) to 22.9%, 34.2%, and 52.9%, respectively. These results confirmed that compound **18** caused G2/M-phase arrest in a concentration dependent manner in HeLa cells.

It is widely known that G2/M transition is regulated principally by

Table 1
Structures of designed compounds and their binding affinity to Plk1 PBD, Plk2 PBD and Plk3 PBD.

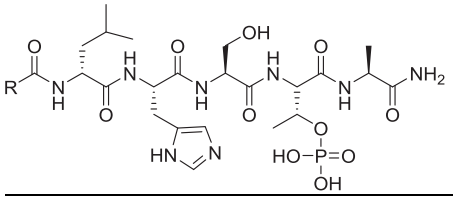

Compound	R	Plk1 PBD IC_{50} (μM)[a]	Plk2 PBD IC_{50} (μM)[a]	Plk3 PBD IC_{50} (μM)[a]
LHSpTA(**6**)	–	9.69	> 100	> 100
7	CH_3–	14.83	ND	ND
8		0.80	> 100	> 100
9		15.97	ND	ND
10		15.44	ND	ND
11		16.87	ND	ND
12		5.07	ND	ND
13		10.43	ND	ND
14	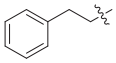	8.08	ND	ND
15	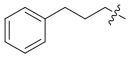	16.69	ND	ND
16		2.40	> 100	> 100
17		1.23	> 100	> 100
18		0.80	> 100	> 100

N.D.: Not Determined.
[a] IC_{50} values represent the mean of at least two independent determinations.

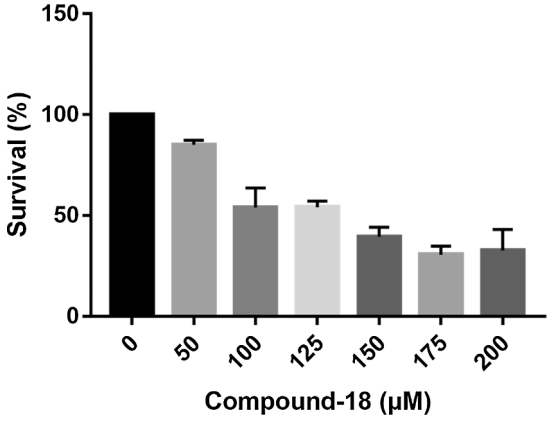

Fig. 2. *In vitro* cell toxicity (MTT) after 24 h incubation with the peptidomimetic **18** on HeLa cancer cells. The data shown represent results from three independent experiments performed in duplicate.

the Cyclin B1-CDK1. Cyclin B1 is essential for the progression of the cells into and out of M phase of the cell cycle. Increasing evidence also indicates that during G2 phase, Cyclin B1-CDK1 complex is held in an inactive state. Therefore, HeLa cells were treated with compound **18** and the expression of the proteins involved in cell cycle was evaluated by western blot. As shown in Fig. 3**C and 3D**, treatment with **18** at concentrations of 50, 100 and 150 μM caused dose dependent decrease in the expression of cyclin B1 and CDK1 in HeLa cells.

2.5. Compound *18* induced the hela cells to undergo cell apoptosis

To further confirm the apoptosis induced by **18**, flow cytometry with the fluorescein isothiocyanate Annexin V/propidium iodide (PI) double-staining assay was carried out to evaluate whether **18**-induced cell death was due to apoptosis or necrosis. As shown in Fig. 4**A and 4B**, after treated with 50, 100 and 150 μM **18** for 24 h, the early and median apoptotic cells (right low section of fluorocytogram) represented 18.7%, 38.2% and 51.1% of the total cells respectively compared to the DMSO group with 0%. To examine the apoptotic events associated with **18**-induced apoptosis, we analyzed the expression of the apoptotic proteins. Results showed that the apoptotic protein PARP cleavage were significantly activated in a dose-dependent manner after the treatment of **18** (50, 100 and 150 μM) for 24 h (Fig. 4**C and 4D**). The Caspase protein is a member of the cysteine-aspartic acid protease (Caspase) family. Sequential activation of Caspase-3 plays a central role in the phase of cell apoptosis. In our assays we found that the expression of Caspase-3 protein didn't change much, however the active form of Caspase-3, cleaved Caspase-3 were significantly increased in a dose-dependent manner after the treatment of **18** (Fig. 4**C and 4D**). These results indicate that induction of apoptosis by **18** is involved in its anti-cancer activity.

2.6. Plasma stability

The stability of the L-peptide **6** and D-amino modified compound **18** following time-dependent incubation in rat plasma were determined using LC-MS. As shown in Fig. 5, the degradation of compound **18** is significantly ($p < 0.05$) slower than compound **6** after 60 min and longer incubation. By 120 min, 52.5% of compound **6** retained in plasma, while > 80% for compound **18** remained in comparison. This result demonstrated that compound **18** have improved stability in rat plasma compared to L-peptide inhibitor LHSpTA (**6**) which confirmed our hypothesis of plasma-stable D-amino acid modification.

3. Conclusion

A new series D-amino acid modified peptidomimetics were identified as novel and selective Plk1 PBD inhibitors. The *in vitro* Plk1 PBD inhibitory activity of the synthesized compounds were evaluated using FP assay. Compounds **8**, **16**, **17** and **18** were significantly active with IC_{50} values ranging from 0.80 to 2.40 μM, and showed excellent selectivity to Plk2 PBD and Plk3 PBD according to the isoform selectivity result. These results confirmed that our newly identified D-amino acid-containing peptidomimetics were potent and selective Plk1 PBD inhibitors.

D-amino acid-containing peptidomimetic **18** inhibited human HeLa cancer cell survival in a dose-dependent manner with an IC_{50} of 122 μM, which implies that **18** is more potent to HeLa cancer cell even than the reported PEGylated version of compound **4** under the same conditions. The cell cycle arrest analysis suggested that compound **18** could cause the G2/M phase cell cycle arrest of HeLa cells in a dose dependent manner. Fluorescein isothiocyanate Annexin V/propidium iodide (PI) double-staining assay and western-blot results indicate that **18** could be a dose-dependent apoptosis inducer in HeLa cells. Additionally, compound **18** had improved stability in rat plasma compared to L-peptide inhibitor LHSpTA (**6**) which confirmed our hypothesis of plasma-stable D-amino acid modification.

In conclusion, this work may provide novel lead compound for the discovery and development of potent, selective and plasma stable Plk1 PBD inhibitors as potential anticancer agents.

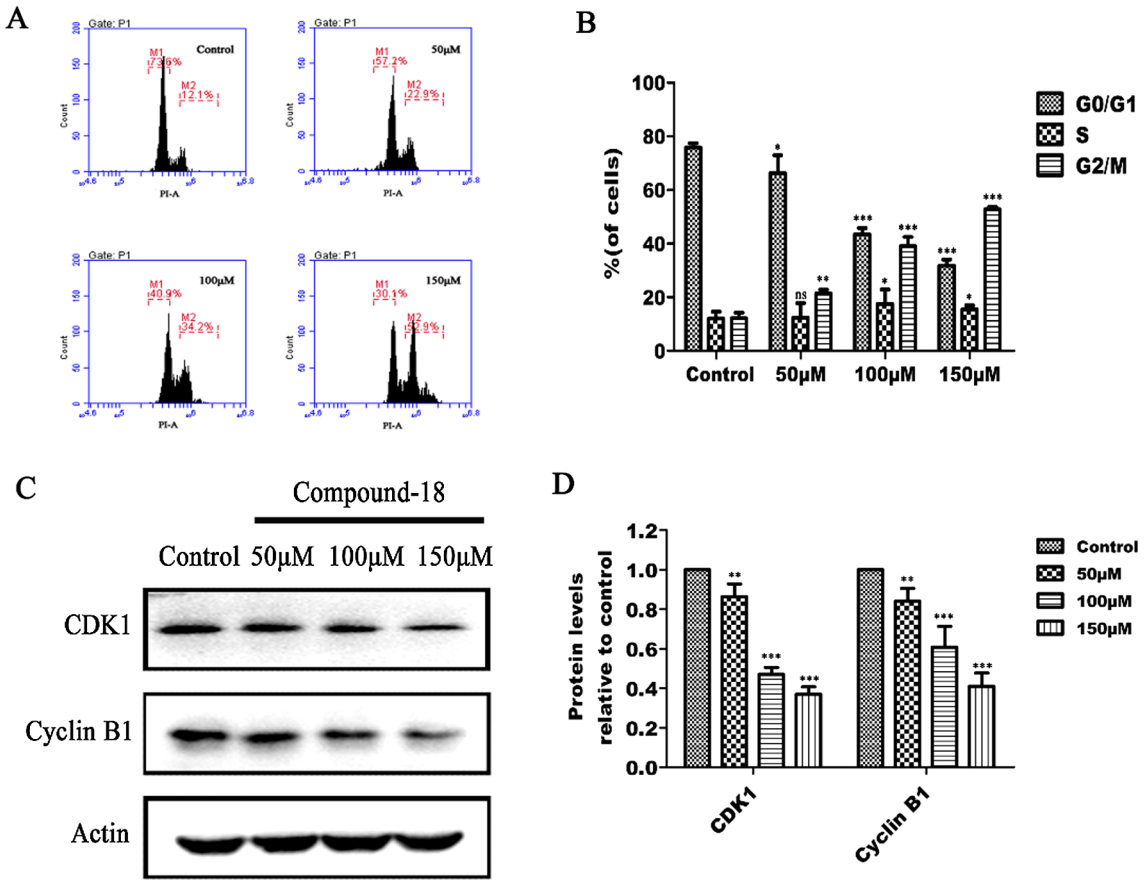

Fig. 3. Investigation of cell cycle distribution in HeLa cells by compound **18**. (A) Effect of **18** (50, 100 and 150 μM) on the cell cycle distribution of HeLa cells after release for 24 h; (B) Quantitative analysis of cell cycle distributions; (C) Western blot analysis of the levels of CDK1, Cyclin B1 expression in HeLa cells treated by **18** (50, 100 and 150 μM) for 24 h. β-actin was used as the control; (D) Quantitative analysis. The relative levels of each signaling event to control β-actin were determined by densimetric scanning. The values shown were the means ± SD (n = 3).

4. Experimental section

4.1. Chemistry

Rink amide 4-methylbenzhydrylamine (MBHA) resin and 9-fluorenylmethoxycarbonyl (Fmoc) amino acids were obtained from Jill Biochemical Co., Ltd. Other reagents used for peptide synthesis included trifluoroacetic acid (TFA; Aladdin Reagent Co., Ltd), piperidine (Sinopharm Chemical Reagent Co., Ltd), 1-*O*-benzotriazole-*N*,*N*,*N*′,*N*′-tetramethyluronium hexafluoro-phosphate (HBTU; Jill Biochemical Co., Ltd), 1-hydroxybenzotriazole hydrate (HOBt; Jill Biochemical Co., Ltd), and *N*,*N*-dimethylformamide (DMF, peptide synthesis grade; Tianjin Chemical Reagent Factory).

Following the synthetic method reported before [13], the designed peptidomimetic were synthesized by Fmoc SPPS methods using Rink amide with an initial loading of 0.82 mmol/g. Fmoc-Ser(*t*-Bu)-OH and other Fmoc protected amino acids were purchased from Jill Biochemical Co., Ltd. Resins were swollen in *N*,*N*-dimethylformamide (DMF) for 30 min before synthesis. Then the Fmoc-protected amino acid (5.0 equiv) was treated with HOBt (5.0 equiv), HBTU (5.0 equiv) and *N*, *N*-diisopropylethylamine (10.0 equiv) in DMF (2 mL) for 2 min for activation. This solution was then added to the free amine on resin, and the reaction for coupling was proceed using vortex stirring for 0.5–1 h. The mixture was then washed with DMF, and Fmoc removed using 20% piperidine in DMF (1 × 5 min, 1 × 15 min). The resin was washed once again, and the process was repeated for the next amino acid, and finally the resin was washed with DMF, methanol, dichloromethane and ether and then dried under vacuum. Linear peptides were cleaved from the resin with 5% triisopropylsilane (TIS) and 5% H_2O in trifluoroacetic acid (TFA, approximately 2 mL of TFA per 100 mg of resin) for 4 h. The cleavage mixture was mixed with cold ether to precipitate the peptide and then centrifugation. Reverse-phase HPLC analysis (RP-HPLC) was carried out on the preparative Vydac C18 column (15 μm, 20 mm × 250 mm) using an appropriate water/acetonitrile gradient in the presence of 0.1% TFA. The final purity of the peptides (> 95%) was assessed by RP-HPLC on an analytical Vydac C_{18} column (4.6 mm × 250 mm, 300 Å, 5 μm particle size). The molecular masses of purified peptides were determined using ESI-MS (Thermo-Finnigan, San Jose, CA, USA).

Peptide **6**. HRMS (ESI-TOF) *m/z* calc'd for $C_{24}H_{41}N_8O_{11}P$ $[M+H]^+$ 649.2666, found 649.2785, 97.41% purity by analytical HPLC;

Peptide **7**. HRMS (ESI-TOF) *m/z* calc'd for $C_{24}H_{41}N_8O_{11}P$ $[M+H]^+$ 649.2666, found 649.2755, 96.29% purity by analytical HPLC;

Peptide **8**. HRMS (ESI-TOF) *m/z* calc'd for $C_{29}H_{48}N_9O_{12}P$ $[M+H]^+$ 746.3225, found 746.3241, 97.37% purity by analytical HPLC;

Peptide **9**. HRMS (ESI-TOF) *m/z* calc'd for $C_{26}H_{43}N_8O_{11}P$ $[M+H]^+$ 675.2822, found 675.2949, 97.55% purity by analytical HPLC;

Peptide **10**. HRMS (ESI-TOF) *m/z* calc'd for $C_{27}H_{45}N_8O_{11}P$ $[M+H]^+$ 689.2979, found 689.3019, 95.25% purity by analytical HPLC;

Peptide **11**. HRMS (ESI-TOF) *m/z* calc'd for $C_{28}H_{47}N_8O_{11}P$ $[M+H]^+$ 703.3135, found 703.3220, 98.67% purity by analytical HPLC;

Peptide **12**. HRMS (ESI-TOF) *m/z* calc'd for $C_{29}H_{49}N_8O_{11}P$ $[M+H]^+$ 717.3292, found 717.3374, 98.58% purity by analytical HPLC;

Peptide **13**. HRMS (ESI-TOF) *m/z* calc'd for $C_{29}H_{43}N_8O_{11}P$ $[M+H]^+$ 711.2822, found 711.3057, 99.45% purity by analytical HPLC;

Peptide **14**. HRMS (ESI-TOF) *m/z* calc'd for $C_{30}H_{45}N_8O_{11}P$ $[M+H]^+$ 725.2979, found 739.3232, 99.36% purity by analytical HPLC;

Peptide **15**. HRMS (ESI-TOF) *m/z* calc'd for $C_{31}H_{47}N_8O_{11}P$ $[M+H]^+$

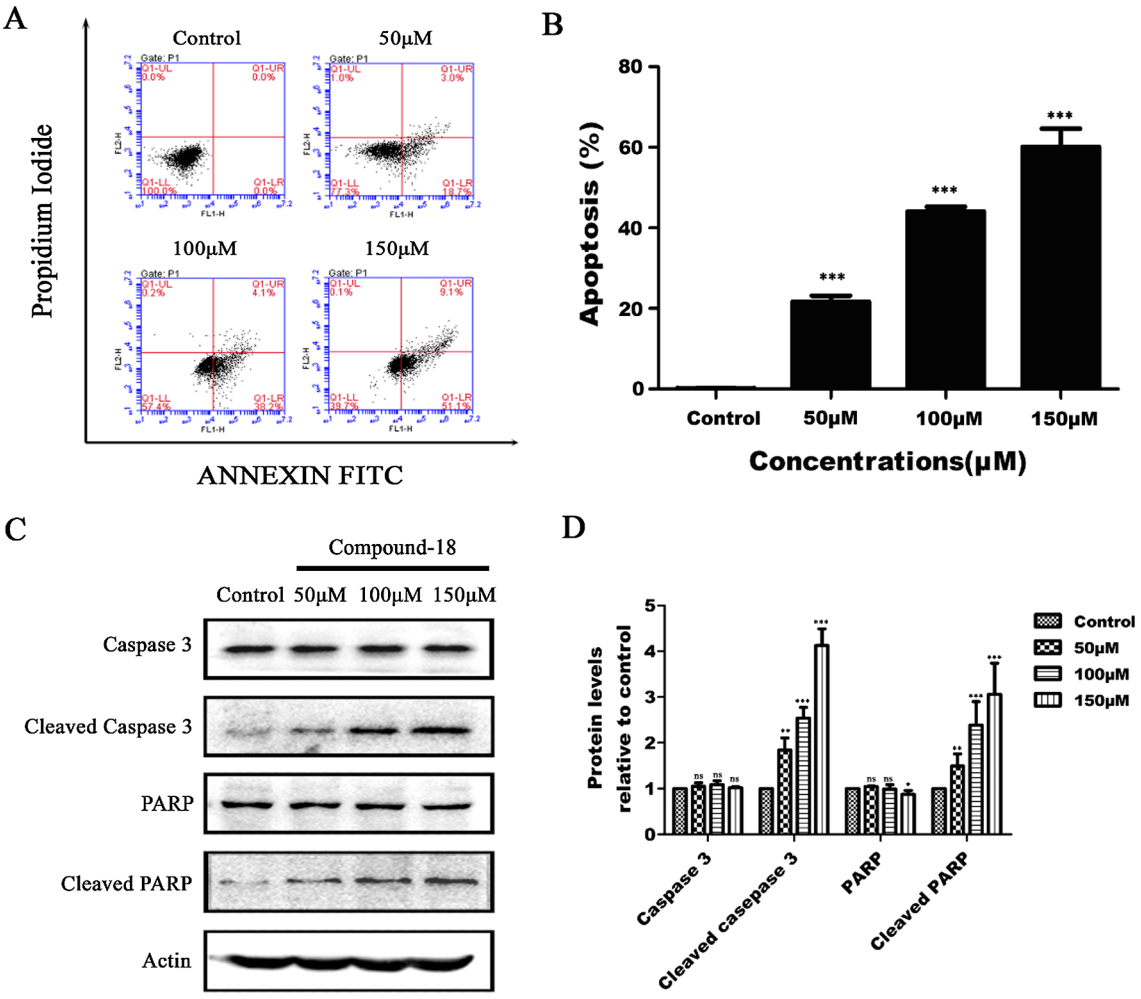

Fig. 4. The apoptotic effects of **18** in HeLa cells. (A) Induction of apoptosis, measured by Annexin V/PI assay following treatment with **18** (50, 100 and 150 μM) for 24 h. Control cells were treated with DMSO alone. (B) The proportion of apoptotic HeLa cells increased dependently with **18** at different concentrations (50, 100 and 150 μM). (C) Effect on PARP and Caspase 3 in HeLa cells after treatment with **18** (50, 100 and 150 μM) for 24 h. (D) The relative levels of each signaling event to control actin were determined by densimetric scanning. The values shown were the means ± SD (n = 3).

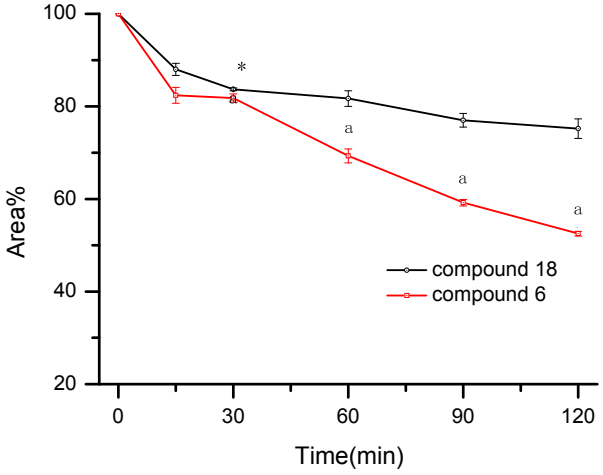

Fig. 5. Stability of compound **6** and **18**. a: statically significant different ($p < 0.05$) for area% of compound **6** and **18**. Data was tested by One-way ANOVA.

739.3135, found 753.3572, 95.91% purity by analytical HPLC;

Peptide **16**. HRMS (ESI-TOF) *m/z* calc'd for $C_{28}H_{42}N_9O_{11}P$ $[M+H]^+$ 712.2796, found 712.2803, 95.86% purity by analytical HPLC;

Peptide **17**. HRMS (ESI-TOF) *m/z* calc'd for $C_{28}H_{42}N_9O_{11}P$ $[M+H]^+$ 712.2795, found 712.2812, 95.57% purity by analytical HPLC;

Peptide **18**. HRMS (ESI-TOF) *m/z* calc'd for $C_{27}H_{41}N_8O_{12}P$ $[M+H]^+$ 701.2674, found 701.2679, 95.43% purity by analytical HPLC.

4.2. Fluorescence polarization (FP) assays

The binding experiments were performed on a SpectraMax MultiMode Microplate Reader (Molecular Devices) using the excitation at 485 nm and emission filters at 535 nm, respectively. In the fluorescein polarization assays, FP was determined by measuring intensities parallel (Intparallel, F∥) and the perpendicular fluorescence intensity (Intperpendicular, F⊥). The percentage inhibition of the phosphopeptides at each concentration was defined as $= 1 - (P_{obs} - P_{min})/(P_{max} - P_{min})$. Where, P_{max} was the polarization of the wells containing Plk1 PBD and the probe, P_{min} was referred to the polarization of the free probe, and the P_{obs} was the polarization for the wells containing the inhibitors at a range of concentrations under the assay conditions [15]. Briefly, FITC-GPMQSpTPLNG-OH was used as the Fluorescein-labeled peptides (fluorescent probe, purity > 95%) as previously reported, which was dissolved in dimethyl sulfoxide (DMSO) and the finally optimized concentration was set at 20 nM [11]. Phosphopeptides used for competition binding assays were dissolved in assay buffer. The buffer makes up 10 mM NaCl, 50 mM Tris (pH 8.0), 1 mM EDTA-2Na. We further performed the sensitivity by synthesizing two new

fluorescent probes, FITC-GPMQTSpTPKNG-OH for Plk2 PBD and FITC-GPLATSpTPKNG-OH for Plk3 PBD, respectively.

Binding-affinities experiments were performed in 384-well, black, round microtiter bottom plates (Corning 3575, Thermo Scientific), which were filled with 20 μL of 60 nM FITC-GPMQSpTPLNG-OH, 20 μL of 4 μM Plk1 PBD, 20 μL of tested phosphopeptides at varying concentrations in assay buffer. A well containing no Plk1 PBD was served as a blank control whereas the negative control including Plk1 PBD, probe complex and assay buffer (equivalent to 0% inhibition). The 384-well black plate was incubated at room temperature for 30 min with gentle shaking prior to FP values measurements. However, the Plk2 PBD or Plk3 PBD was introduced into the selectivity assays to replace Plk1 PBD. All experiments were performed in triplicate. Competition binding data were analyzed using GraphPad Prism 6.0 software (GraphPad Software, San Diego, CA) and the inhibition constants (IC_{50}) were calculated by nonlinear curve fitting.

4.3. In vitro cancer cell line proliferation inhibition assay

In this study, human cancer cell line HeLa was introduced into each well of a 96-well plate, with a density of 2500 cells/well. The cells were then exposed to compound **18** of different concentrations (50, 100, 125, 150, 175, 200 μM) (100 μL/well). Controls were performed in which only culture media was added into wells containing cells. After 24 h incubation, 5 mg/ml 3-(4,5-Dimethylthiazol-2-yl)-2,5-diphenyl tetrazolium bromide (MTT) solution (20 μL/well) was added and cultured for 4 h, and then the supernatant was discarded and dimethyl sulfoxide (DMSO) was added in (100 μL/well), respectively. The suspension was placed on micro-vibrator for 5 min and the absorbance (A) was measured at 570 nm by the Universal Microplate Reader (EL800, BIO-TEK INSTRUMENTS INC.). Triplicate experiments were performed in a parallel manner for each concentration point and the results were reported as mean. Cell inhibitory ratio was calculated by the following formula:

$$\text{Inhibitory Ratio}(\%) = [(A_{control} - A_{treated})/A_{control}] \times 100\%$$

The IC_{50} was taken as the concentration that caused 50% inhibition of cell proliferation.

4.4. Cell cycle arrest in HeLa cells

HeLa cells (1×10^6) were incubated at 37 °C overnight. Different concentrations of **18** (50, 100 and 150 μM) were added to the plate and incubated for 24 h. Afterwards, HeLa cells were harvested by gently adding trypsin and collected by centrifugation at 1000 g for 5 min. The cells were washed twice with ice-cold PBS, and fixed gently in 70% ice-cold ethanol at 4 °C overnight. Subsequently, the cells were stained with a solution containing 500 μL, 10 μL propidium iodide (PI) and 10 μL RNase A in a dark room for 30 min at 37 °C. Finally, the percentage of stained cells in G2/M was analyzed using the fluorescence activated cell sorting analysis (BD Biosciences, San Jose, CA) and the results were analyzed by Mod Fit LT3.0 software (Dako Colorado, Inc.).

4.5. Annexin V/PI double-staining assay

Hela cells (1×10^6 cells/mL) were treated with **18** (50, 100 and 150 μM) for 24 h, harvested, and then washed and resuspended with PBS. Apoptotic cells were quantified by annexin V-FITC-PI double staining, using a kit purchased from Bipec, according to the manufacturer's instructions. Flow cytometric analysis was performed immediately after supravital staining. Data acquisition and analysis were performed with FACSCalibur and CellQuest software.

4.6. Western blot analysis

The effect of **18** treatment on the expression of the CDK1, Cyclin B1, Caspase-3 and apoptotic protein PARP was determined. HeLa cells were incubated with **18** at 50, 100 and 150 μM concentrations for 24 h. Cells were collected and lysed in lysis buffer (50 mM Tris-Cl, pH 7.6, 150 mM NaCl, 1 mM EDTA, 1% (m/v) NP-40, 0.2 mM PMSF, 0.1 mM NaF and 1.0 mM DTT). The lysates were clarified by centrifugation at 4 °C for 15 min at 13,000g. The protein concentration was determined with the BCA reagent. Equal amounts of protein were subjected to electrophoresis on 10% SDS-polyacrylamide gels and transferred onto the PVDF membranes (Millipore, Boston, MA). The blots were incubated with appropriate primary antibodies overnight at 4 °C followed by IRDyeTM800 conjugated secondary antibody for 1 h at 37 °C. Detection was performed by the Odyssey Infrared Imaging System (LI-COR Inc., USA). All blots were stripped and reprobed with polyclonal anti-β-actin antibody to ascertain equal loading of proteins.

4.7. Plasma stability

One milliliter of rat plasma was mixed with 0.1 mL compound **6** or compound **18** solution to make a final concentration of 10 μg mL^{-1}. The mixture was incubated at 37 ℃. An aliquot of 100 μL solution was taken at different time interval and mixed with 300 μL of methanol acetonitrile (50:50, v/v) to precipitate plasma proteins. After vortexed and centrifuged at 4 ℃ for 20 min at 12,000 rpm. The supernatant was transferred and determined with LC-MS.

The LC-MS analysis was performed by a Thermo TSQ Quantis LC-MS/MS system (Thermo, US), consisting of a binary pump solvent management system, an online degasser, an autosampler, and a TSQ Quantum mass spectrometry. The chromatographic separation was performed with an InertSustain C18 column (150 × 4.6 mm, 5 μm) with a gradient mobile phase of 0.1% formic acid in water (solvent A) and 0.1% formic acid in acetonitrile (solvent B). The gradient program was as follows: 0 min 5% B; 8 min 30% B; 8.2 min 80% B; 9 min 80% B; 9.1 min 5% B; 15 min 5% B, and the flow rate was 1 mL min^{-1}. All the samples were studied with an injection volume of 20 μL.

Positive electrospray ionization (ESI) mode was used for the MS determination, with the source parameters were as follows: spray voltage, 4000 V; transfer tube temperature, 350 °C; sheath gas 30 Arb; ion sweep gas pressure 1.0 psi.

Acknowledgements

This work has been financially supported by National Natural Science Foundation of China (No. 81573278) and Excellent Science and Technology Innovation Team Projects of Jiangsu Province Universities in 2017.

Appendix A. Supplementary material

Supplementary data to this article can be found online at https://doi.org/10.1016/j.bioorg.2019.02.022.

References

[1] J.E. Park, N.K. Soung, Y. Johmura, Y.H. Kang, C. Liao, K.H. Lee, C.H. Park, M.C. Nicklaus, K.S. Lee, Polo-box domain: a versatile mediator of polo-like kinase function, Cell. Mol. Life Sci. 67 (2010) 1957–1970.
[2] J. Luo, M.J. Emanulele, D. Li, C.J. Creiquton, M.R. Schlabach, T.F. Westbrook, K.K. Wong, S.J. Elledge, A genome-wide RNAi screen identifies multiple synthetic lethal interactions with the Ras oncogene, Cell 137 (2009) 835–848.
[3] K. Strebhardt, A. Ullrich, Targeting polo-like kinase 1 for cancer therapy, Nat. Rev. Cancer 6 (2006) 321–330.
[4] D.M. Lowery, D. Lim, M.B. Yaffe, Structure and function of Polo-like kinases, Oncogene 24 (2005) 248–259.
[5] Y.J. Jang, C.Y. Lin, S. Ma, R.L. Erikson, Functional studies on the role of the C-terminal domain of mammalian polo-like kinase, Proc. Natl. Acad. Sci. USA 99 (2002) 1984–1989.
[6] S.M. Yun, T. Moulaei, D. Lim, J.K. Bang, J.E. Park, S.R. Shenoy, F. Liu, Y.H. Kang, C. Liao, N.K. Soung, S. Lee, D.Y. Yoon, Y. Lim, D.H. Lee, A. Otaka, E. Appella, J.B. Mcmahon, M.C. Nicklaus, T.R. Burke Jr., M.B. Yaffe, A. Wlodawer, K.S. Lee,

Structural and functional analyses of minimal phosphopeptides targeting the polo-box domain of polo-like kinase 1, Nat. Struct. Mol. Biol. 16 (2009) 876–882.
[7] F. Liu, J.E. Park, W.J. Qian, D. Lim, M. Garber, M.B. Yaffe, K.S. Lee, T.R. Burke Jr., Serendipitous alkylation of a Plk1 ligand uncovers a new binding channel, Nat. Chem. Biol. 7 (2011) 595–601.
[8] R.N. Murugan, J.E. Park, E.H. Kim, S.Y. Shin, C. Cheong, K.S. Lee, J.K. Bang, Plk1-targeted small molecule inhibitors: molecular basis for their potency and specificity, Mol. Cells 232 (2011) 209–220.
[9] F. Liu, J.E. Park, W.J. Qian, D. Lim, A. Scharow, T. Berg, M.B. Yaffe, K.S. Lee, T.R. Burke Jr., Identification of high affinity polo-like 1 (Plk1) polo-box domain binding peptides using oxime-based diversification, ACS Chem. Biol. 7 (2012) 805–810.
[10] F. Liu, J.E. Park, W.J. Qian, D. Lim, A. Scharow, T. Berg, M.B. Yaffe, K.S. Lee, T.R. Burke Jr., Peptoid-peptide hybrid ligands targeting the polo box domain of polo-like kinase 1, ChemBioChem 13 (2012) 1291–1296.
[11] R.N. Murugan, J.E. Park, D. Lim, M. Ahn, C. Cheong, T. Kwon, K.Y. Nam, S.H. Choi, B.Y. Kim, D.Y. Yoon, M.B. Yaffe, D.Y. Yu, K.S. Lee, J.K. Bang, Development of cyclic peptomer inhibitors targeting the polo-box domain of polo-like kinase 1, Bioorg. Med. Chem. 21 (2013) 2623–2634.
[12] X.Z. Zhao, D. Hymel, T.R. Burke Jr., Application of oxime-diversification to optimize ligand interactions within a cryptic pocket of the polo-like kinase 1 polo-box domain, Bioorg. Med. Chem. Lett. 26 (2016) 5009–5012.
[13] M. Ahn, Y.H. Han, J.E. Park, S. Kim, W.C. Lee, S.J. Lee, P. Gunasekaran, C. Cheong, S.Y. Shin Sr., H.Y. Kim, E.K. Ryu, R.N. Murugan, N.H. Kim, J.H. Bang, A new class of peptidomimetics targeting the polo-box domain of polo-like kinase 1, J. Med. Chem. 58 (2015) 294–304.
[14] W.J. Qian, J.E. Park, K.S. Lee, T.R. Burke Jr., Non-proteinogenic amino acids in the pThr-2 position of a pentamer peptide that confer high binding affinity for the polo box domain (PBD) of polo-like kinase 1 (Plk1), Bioorg. Med. Chem. Lett. 22 (2012) 7306–7308.
[15] X.Z. Zhao, D. Hymel, T.R. Bruke Jr., Enhancing polo-like kinase 1 selectivity of polo-box domain-binding peptides, Bioorg. Med. Chem. 25 (2017) 5041–5049.
[16] D. Hymel, T.R. Burke Jr., Phosphatase-stable phosphoamino acid mimetics that enhance binding affinities with the polo-box domain of polo-like kinase 1, ChemMedChem 12 (2017) 202–206.
[17] M. Liu, C. Li, M. Pazgiera, C. Li, Y. Mao, Y. Lv, B. Gu, G. Wei, W. Yuan, C. Zhan, W. Lu, W. Lu, D-peptide inhibitors of the p53–MDM2 interaction for targeted molecular therapy of malignant neoplasms, Proc. Natl. Acad. Sci. USA 107 (2010) 14321–14326.
[18] A.M. Torres, I. Menz, P.F. Alewood, P. Bansal, J. Lahnstein, C.H. Gallagher, P.W. Kuchel, D-amino acid residue in the C-type natriuretic peptide from the venom of the mammalOrnithorhynchus anatinus, the Australian platypus, FEBS Lett. 524 (2002) 172–176.
[19] S.M. Miller, R.J. Simon, S. Ng, R.N. Zuckermann, J.M. Kerr, W.H. Moos, Comparison of the proteolytic susceptibilities of homologous L-amino acid, D-amino acid, and N-substituted glycine peptide and peptoid oligomers, Drug Dev. Res. 35 (1995) 20–32.
[20] R.C.D. Milton, S.C.F. Milton, S.B.H. Kent, Total chemical synthesis of a D-enzyme: the enantiomers of HIV-1 protease show reciprocal chiral substrate specificity, Science 256 (1992) 1445–1448.
[21] M.C. Lu, Z.Y. Chen, Y.L. Wang, Y.B. Jiang, Z.W. Yuan, Q.D. You, Z.Y. Jiang, Binding thermodynamics and kinetics guided optimization of potent Keap1-Nrf2 peptide inhibitors, RSC Adv. 5 (2015) 85983–85987.